Energy Levels in Ho^{166}

GORDON L. STRUBLE,* JEAN KERN,† AND RAYMOND K. SHELINE‡
Departments of Chemistry and Physics, Florida State University, Tallahassee, Florida
(Received 3 August 1964)

The energy levels in Ho^{166} are studied by means of (d,p) reaction spectroscopy and a Q value of 4025 ± 7 keV is obtained for the ground state. A rotational model is used to interpret the energies and generate state vectors for the experimental levels. Using these vectors and the distorted-wave Born approximation, a theoretical (d,p) spectrum is constructed and compared with the experimental data.

I. INTRODUCTION

ALTHOUGH the low-energy-level structure of deformed even-even and odd-A nuclei has been extensively studied, only within the past several years has it been possible to experimentally study odd-odd deformed nuclei in detail. These odd-odd nuclei are among the most interesting nuclei theoretically because interactions between the odd particles have a strong influence on the energies of the low-lying states.

Ho^{166} has probably been studied better than any of the other odd-odd deformed nuclei in the rare-earth region of the nuclear periodic table. Three groups have independently studied the decay[1–3] of Dy^{166}, and two other groups have reported results of (n,γ) studies.[4,5] A compilation of these data is shown in Fig. 3.

Since the level densities in odd-odd nuclei are generally large when collective motion is prominent, a successful study requires high-energy resolution. The Florida State University Tandem Van de Graaff accelerator in conjunction with a Browne-Buechner broad-range magnetic spectrograph[6] was used in these experiments and provided a resolution of from 8 to 23 keV. Because of the complexity of the data, which is due to high level densities, a nonlinear least-squares analysis was essential for the interpretation.

These experiments have yielded level schemes and relative cross sections. Second-order interactions involving angular momentum of the particles and the total angular momentum as well as the quantitatively unknown particle-particle interaction cause the interpretation of the data to be complex. The theoretical analysis consists of predicting the level structure from the known spectra of neighboring isotopic and isotonic odd-A nuclei. Then using parameters that depend on the detailed single-particle structure of the nucleus, the rotational Hamiltonian is diagonalized in a direct product basis $D_{MK}{}^{I}\chi_{\Omega_1}\chi_{\Omega_2}$ after proper symmetrization. χ_{Ω_i}, $i=1$, 2 are the Nilsson wave functions.[7] From the state vectors generated, theoretical cross sections are calculated using distorted wave reaction theory.[8] A comparison between the theoretical results and experimental data is then attempted with the intention of deducing the nature of the low-energy structure.

II. THEORY

The coupling model for odd-A nuclei of Bohr, Mottelson, Nilsson, and Kerman[7,9,10] has been successful in explaining the spectra of odd-A deformed nuclei.[11] In an extension of this model to odd-odd nuclei, two particles coupled to a deformed core must be considered. If the interaction energy between the two nucleons is small compared to the energy with which each is bound to the core, then a simple extension of the odd-A model can be made and the interaction energy can later be treated as a perturbation. With these assumptions the model Hamiltonian may be written

$$H=H_R+H_{\mathrm{RPC}}+H_P(p)+H_P(n)+H_{\mathrm{INT}}, \qquad (1)$$

where

$$H_R=(1/2\Im)[\mathbf{I}\cdot\mathbf{I}-I_3{}^2],$$

$$H_{\mathrm{RPC}}=-(1/\Im)[I_1j_1(p)+I_2j_2(p)+I_1j_1(n)+I_2j_2(n)-j_1(p)j_1(n)-j_2(p)j_2(n)],$$

* Present address: Lawrence Radiation Laboratory, University of California, Berkeley, California.
† Supported in part by the "Fonds National Suisse de la recherche scientifique."
‡ Supported in part by the U. S. Atomic Energy Commission Contract No. AT-(40-1)-2434, the U. S. Air Force Contract No. AF-AF0SR-440-63 and the Nuclear Program of the State of Florida.

[1] R. G. Helmer and S. B. Burson, Phys. Rev. **119**, 788 (1960).
[2] R. Gunnink (private communication).
[3] J. S. Geiger, R. L. Graham, and G. T. Ewan, Bull. Am. Phys. Soc. **3**, 255 (1960).
[4] I. V. Estulin, A. S. Melioransky, and L. F. Kalinkin, Nucl. Phys. **24**, 118 (1961).
[5] H. T. Motz and E. T. Jurney, Bull. Am. Phys. Soc. **9**, 31 (1964).
[6] C. P. Browne and W. W. Buechner, Rev. Sci. Instr. **27**, 899 (1956).
[7] S. G. Nilsson, Kgl. Danske Videnskab. Selskab, Mat.-Fys. Medd. **29**, No. 16 (1955).
[8] R. H. Bassel, R. M. Drisko, and G. R. Satchler, Atomic Energy Commission Report ORNL-3240 (unpublished).
[9] A. Bohr and B. R. Mottelson, Kgl. Danske Videnskab. Selskab, Mat.-Fys. Medd. **27**, No. 16 (1953).
[10] A. K. Kerman, Kgl. Danske Videnskab. Selskab, Mat.-Fys. Medd. **30**, No. 15 (1956).
[11] B. R. Mottelson and S. G. Nilsson, Kgl. Danske Videnskab. Selskab. Mat.-Fys. Skrifter **1**, No. 8 (1959).

$$H_P(p)=\frac{j_1^2(p)+j_2^2(p)}{2\Im}+\frac{\mathbf{p}^2(p)}{2M(p)}+V(\mathbf{r}(p))$$
$$=\frac{j_1^2(p)+j_2^2(p)}{2\Im}+H_P'(p),$$
$$H_P(n)=\frac{j_1^2(n)+j_2^2(n)}{2\Im}+\frac{\mathbf{p}^2(n)}{2M(n)}+V(\mathbf{r}(n))$$
$$=\frac{j_1^2(n)+j_2^2(n)}{2\Im}+H_P'(n),$$
$$H_{\rm INT}=V_{\rm interaction}.$$

If $H_{\rm INT}$ and $H_{\rm RPC}$ are neglected, then H_R, $H_P(p)$, and $H_P(n)$ are mathematically uncoupled, and an eigenvector of the Hamiltonian can be written as a direct product

$$\psi_{IMK}=\phi_{IMK}\Phi_{\Omega_1}(p)\Phi_{\Omega_2}(n),\quad K=|\Omega_1\pm\Omega_2|. \tag{2}$$

The Ω_i, $i=1, 2$, are the projections of the particle angular momentum on the 3-axis. That $K=|\Omega_1\pm\Omega_2|$ is a result of the assumption of axial symmetry.

After expanding the single-particle vectors, (2) can be rewritten

$$\psi_{IMK}=\phi_{IMK}\sum_{j_1}C_{j_1}\chi_{\Omega_1}{}^{j_1}(p)\sum_{j_2}C_{j_2}\chi_{\Omega_2}{}^{j_2}(n),$$
$$K=|\Omega_1\pm\Omega_2|. \tag{3}$$

However, (3) must be symmetrized since a rotation of 180° about the 2-axis must change only the phase of a state vector. The same is true for an arbitrary rotation about the 3-axis. The state vector is then

$$\psi_{IMK}=\frac{1}{\sqrt{2}}\sum_{j_1}\sum_{j_2}C_{j_1}C_{j_2}[\chi_{\Omega_1}{}^{j_1}(p)\chi_{\Omega_2}{}^{j_2}(n)\phi_{IMK}$$
$$+(-1)^{I-j_1-j_2}\chi_{-\Omega_1}{}^{j_1}(p)\chi_{-\Omega_2}{}^{j_2}(n)\phi_{IM-K}],$$
$$K=|\Omega_1\pm\Omega_2|. \tag{4}$$

In this representation $H_R+H_P'(p)+H_P'(n)$ is diagonal and

$$(\psi_{IMK},[H_R+H_P'(p)+H_P'(n)]\psi_{IMK})$$
$$=(\hbar^2/2\Im)[I(I+1)-K^2]$$
$$+E_P(p)+E_P(n),\quad K=|\Omega_1\pm\Omega_2|. \tag{5}$$

It is clear that there will be a difference in rotational energy depending on whether $K=\Omega_1+\Omega_2$ or $K=|\Omega_1-\Omega_2|$. For the case $I=K=\Omega_1+\Omega_2$, the rotational energy is

$$W_{\rm rot}=(\hbar^2/2\Im)(\Omega_1+\Omega_2), \tag{6}$$

while for the case $I=K=|\Omega_1-\Omega_2|$

$$W_{\rm rot}=(\hbar^2/2\Im)|\Omega_1-\Omega_2|. \tag{7}$$

Thus the state having $K=|\Omega_1-\Omega_2|$ will have the lower energy, and that having $K=(\Omega_1+\Omega_2)$ will appear at an energy

$$\Delta W_{\rm rot}=(\hbar^2/\Im)\Omega_l \tag{8}$$

above it, where Ω_l is the smaller of Ω_1 and Ω_2.

Consider the effect of $H_{\rm RPC}$ on the energies and vectors. For the diagonal matrix elements

$$(\psi_{IMK},H_{\rm RPC}\psi_{IMK}) \tag{9}$$

must be evaluated. Using the explicit form of ψ_{IMK}, the following result is obtained

$$(\psi_{IMK},H_{\rm RPC}\psi_{IMK})$$
$$=(\psi_{IMK},[(1/\Im)[j_1(p)j_1(n)+j_2(p)j_2(n)]]\psi_{IMK})$$
$$=(-1)^{I+1}(1/2\Im)a_1a_2\delta_{K,0}\delta_{|\Omega_1|,1/2}, \tag{10}$$

where

$$a_i=\sum_{j_i}(-1)^{j_i-1/2}|C_{j_i}|^2(j_i+\tfrac{1}{2})\quad i=1, 2, \tag{11}$$

and are called the decoupling parameters of particles which are in single-particle states labeled 1 and 2. The expression for the energies of states within a $K=0$ band must then be modified to read

$$E=(\hbar^2/2\Im)[I(I+1)+(-1)^{I+1}a_1a_2\delta_{|\Omega_1|,1/2}]. \tag{12}$$

$H_{\rm RPC}$ might be expected to support matrix elements between states having the same spin but with $|\Delta K|=1$. Thus it is important to evaluate matrix elements of the form

$$(\psi_{IMK+1},H_{\rm RPC}\psi_{IMK}). \tag{13}$$

The state vectors may be written

$$\psi_{IMK+1}=\frac{1}{\sqrt{2}}\sum_{j_1}\sum_{j_2}C_{j_1\Omega'_1}C_{j_2\Omega'_2}[\chi_{\Omega'_1}{}^{j_1}(p)\chi_{\Omega'_2}{}^{j_2}(n)$$
$$\times\phi_{IMK+1}+(-1)^{I-j_1-j_2}\chi_{-\Omega'_1}{}^{j_1}(p)\chi_{-\Omega'_2}{}^{j_2}(n)$$
$$\times\phi_{IM-(K+1)}],\quad K+1=|\Omega_1'\pm\Omega_2'|, \tag{14}$$

and

$$\psi_{IMK}=\frac{1}{\sqrt{2}}\sum_{j_1}\sum_{j_2}C_{j_1\Omega_1}C_{j_2\Omega_2}$$
$$\times[\chi_{\Omega_1}{}^{j_1}(p)\chi_{\Omega_2}{}^{j_2}(n)\phi_{IMK}+(-1)^{I-j_1-j_2}\chi_{-\Omega_1}{}^{j_1}(p)$$
$$\times\chi_{-\Omega_2}{}^{j_2}(n)\phi_{IM-K}],\quad K=|\Omega_1\pm\Omega_2|. \tag{15}$$

Using backward commutation relations for $\mathbf{I}$, it is readily shown that

$$(\psi_{IMK+1},H_{\rm RPC}\psi_{IMK})$$
$$=-(\hbar^2/2\Im)[I(I+1)-K(K+1)]^{1/2}$$
$$\times\textstyle\sum_{j_1}\sum_{j_2}C_{j_1\Omega_1'}{}^*C_{j_1\Omega_1}C_{j_2\Omega'_2}{}^*C_{j_2\Omega_2}$$
$$\times\{[(j_1-\Omega_1)(j_1+\Omega_1+1)]^{1/2}\delta_{\Omega'_2,\Omega_2}\delta_{\Omega'_1,\Omega_{1+1}}$$
$$+[(j_2-\Omega_2)(j_2+\Omega_2+1)]^{1/2}\delta_{\Omega'_1,\Omega_1}\delta_{\Omega'_2,\Omega_2+1}$$
$$+(-1)^{I-j_1-j_2}[(j_1-\Omega_1)(j_1+\Omega_1+1)]^{1/2}$$
$$\times\delta_{K,0}\delta_{\Omega'_1,-\Omega_1+1}\delta_{\Omega'_2,-\Omega_2}$$
$$+(-1)^{I-j_1-j_2}[(j_2-\Omega_2)(j_2+\Omega_2+1)]^{1/2}$$
$$\times\delta_{K,0}\delta_{\Omega_2',-\Omega_2+1}\delta_{\Omega'_1,-\Omega_1}\}. \tag{16}$$

Finally the H_{RPC} terms can be expected to support matrix elements of the form

$$(\psi_{IMK'}, H_{\mathrm{RPC}}\psi_{IMK}), \tag{17}$$

where $K'=|\Omega_1'\pm\Omega_2'|$, $K=|\Omega_1\pm\Omega_2|$, and $K=K'$. If the state vectors are written

$$\psi_{IMK'}=\frac{1}{\sqrt{2}}\sum_{j_1}\sum_{j_2} C_{j_1\Omega'_1}C_{j_2\Omega'_2}[\chi_{\Omega_1'}{}^{j_1}(p)\chi_{\Omega'_2}{}^{j_2}(n)\phi_{IMK'} +(-1)^{I-j_1-j_2}\chi_{-\Omega'_1}{}^{j_1}(p)\chi_{-\Omega'_2}{}^{j_2}(n)\phi_{IM-K'}], \tag{18}$$

$$\psi_{IMK}=\frac{1}{\sqrt{2}}\sum_{j_1}\sum_{j_2} C_{j_1\Omega_1}C_{j_2\Omega_2}[\chi_{\Omega_1}{}^{j_1}(p)\chi_{\Omega_2}{}^{j_2}(n)\phi_{IMK} +(-1)^{I-j_1-j_2}\chi_{-\Omega_1}{}^{j_1}(p)\chi_{-\Omega_2}{}^{j_2}(n)\phi_{IM-K}], \tag{19}$$

then

$$\begin{aligned}(\psi_{IMK'}, H_{\mathrm{RPC}}\psi_{IMK}) &= \frac{\hbar^2}{2\Im}\sum_{j_1}\sum_{j_2} C_{j_1\Omega'_1}{}^{*}C_{j_1\Omega_1}C_{j_2\Omega'_2}{}^{*}C_{j_2\Omega_2} \\ &\times[(j_1\mp\Omega_1)(j_1\pm\Omega_1+1)]^{1/2} \\ &\times[(j_2\pm\Omega_2)(j_2\mp\Omega_2+1)]^{1/2} \\ &\times\delta_{\Omega'_1,\,\Omega_1\pm1}\delta_{\Omega'_2,\,\Omega_2\mp1}\delta_{K',K} \\ &+(-1)^{I-j_1-j_2}[(j_1\pm\Omega_1)(j_1\mp\Omega_1+1)]^{1/2} \\ &\times[(j_2\mp\Omega_2)(j_2\pm\Omega_2+1)]^{1/2} \\ &\times\delta_{\Omega'_1,\,-\Omega_1\pm1}\delta_{\Omega'_2,\,-\Omega_2\mp1}\delta_{K',K}\delta_{K,0}].\end{aligned} \tag{20}$$

If two bands satisfying the condition $\Delta K=0$ or $|\Delta K|=1$, subject to the appropriate restrictions, are sufficiently far apart in energy to justify second-order perturbation theory, then any effect on the energy levels can be compensated by renormalizing the moment of inertia of the bands, except for $K=0$. In certain cases, it is possible for the odd and even members of the bands to have different moments of inertia. An unusual case occurs if a $K=0$ band is formed from the coupling of a proton and neutron each of whose Ω has a value of $\frac{1}{2}$. Then the $K=1$ band formed by the recoupling of these nucleons will perturb the $K=0$ band, and the moment of inertia of the even members of the bands will be different from the moments of inertia of the odd members.

In the previous discussion, nothing was mentioned about H_{INT}. This term in the Hamiltonian is the most complicated and, at the same time, the most important term to specify since it must describe the effective proton-neutron interaction. In these calculations, the effect of H_{INT} was chosen to be a free parameter. (See Sec. IV.) However, we are at present engaged in computing its effects assuming both central and central-plus-tensor components in the interaction potential.

III. EXPERIMENT

The experiments discussed in this paper were performed at the Florida State University Nuclear Research Institute using a Tandem Van de Graaff accelerator to produce a monochromatic deuteron beam and a Browne-Buechner type magnetic spectrograph[6] to analyze reaction products. Reaction products were detected on an array of four 2 in. by 10 in. fifty-micron nuclear emulsion plates manufactured by the Eastman Kodak Company. These plates were covered with aluminum foil 0.005 in. thick in order to stop elastically scattered deuterons. After exposures of six to ten thousand microcoulombs, the protons were counted in $\frac{1}{2}$ mm strips. The results are displayed as a graph of the number of particles versus plate distance.

Both holmium metal and oxide were used for holmium targets. The metal was evaporated from a tantalum boat onto thin carbon backings and an electron gun was used to evaporate the holmium oxide.

Exposures at 35, 45, 60, 65, 90, and 95° have been performed. The details of the experiments are given in Table I. The 45° spectrum was selected as representative of the several experiments and is shown in Fig. 1.

TABLE I. A summary of experiments for levels in Ho^{166}.

Experiment number	Angle	Target	Bombarding energy	Exposure in microcoulombs
1	35°	oxide	12 MeV	8000
2	45°	metal	12 MeV	8000
3	60°	oxide	11 MeV	10 000
4	65°	metal	12 MeV	7000
5	90°	oxide	11 MeV	10 000
6	95°	oxide	11 MeV	6000

The level density is such that very few peaks, if any, are completely resolved. Thus it was necessary to use a nonlinear least-squares analysis to determine the individual components of the spectrum.[12] Such an analysis was done on the 45 and 95° spectra in the excitation range 140- to 1660-keV excitation and on the 65° spectrum between 140 and 610 keV. The resolution (defined as the full width at half-maximum) is 8 keV at 65°, 10.7 keV at 45°, and 13 keV at 95°. The poorer resolution at 95° explains the lack of observation of some weak peaks that appeared in the 45 and 65° analysis. The shape of the line profile was inferred from the most prominent peaks. The function fitted to the data was a sum of components, each a skew-Gaussian with a tail, but the minimum value for the weighted sum of squares of deviation was obtained with zero skewness and a very small amplitude for the tail. The same functional form has been found in the analysis of some isotopes having a smaller level density. As there is no evidence

[12] R. H. Moore and R. K. Zeigler, Atomic Energy Commission Report LA-2367 (unpublished).

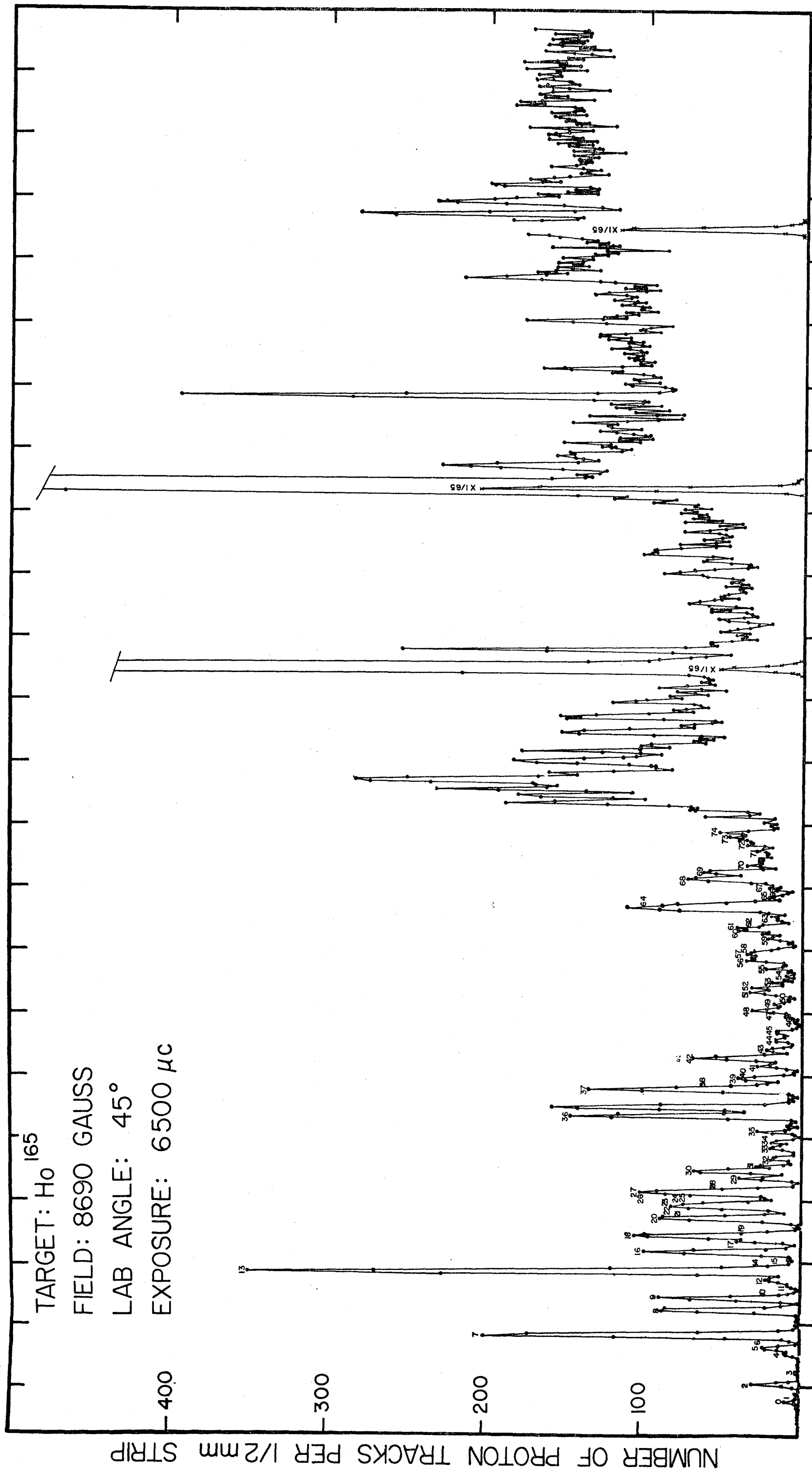

FIG. 1. Proton spectrum from the reaction $Ho^{165}(d,p)Ho^{166}$ at 45°.

that the resolution varies with energy on the range of the analysis, the width of the Gaussian was held constant at each angle.

In Fig. 2 the results of a least-squares analysis on a portion of the 65° spectrum is shown. As can be seen from this figure, there seem to be some intense impurity peaks in this run. The good resolution still makes it valuable. The chosen Gaussian profile is able to fit satisfactorily most peak groups in spite of their sometimes strange contour.

With the position and area estimates for the peaks in the several experiments obtained by least-squares analysis, the Q values for the states are determined from their position along the focal surface using an empirical energy calibration. This calibration was done with α particles from a Po^{210} source and it determined the radius of the charged particle trajectory for a given distance along the focal curve. Impurity peaks are determined from their kinematic shifts relative to the states of the isotope in question. Frequently it is also possible to determine their origin from known Q values. More details of the general experimental procedure are given in a recent publication by Kenefick and Sheline.[13]

Below 130 keV, the observed states have very small cross sections. A long exposure with a much thicker target was therefore taken at 90°, which gave a resolution of 23 keV. This measurement and the 95° measurement were graphically analyzed using a simple triangle shape as the window curve. The fit was considered satisfactory when the scatter of data points about the function was random and the area enclosed by the data points outside the fitted function was approximately

TABLE II. $Ho^{165}(d,p)Ho^{166}$ results. (Energies in keV.)

Level No.	Level energy 45°	Level energy 65°	Level energy 90°	Level energy 95°	Level energy (mean)	Spin, parity, K	Intensity 45°	Intensity 65°	Intensity 90°	Intensity 95°	Comments
0			0.0±3	0.0±3	0 ±3	0−, 0			2.5±1	3±1	
1			10.1±3	7.6±2	9 ±3	7−, 7			4.5±1	6±2	
2	51.1±2		54.1±3	54.5±5	53 ±2	2−, 0	10 ±1		5.5±1	5±2	
3	83.2±2		86.4±7	77.0±5	82 ±3	1−, 0	0.6±0.4		3.0±1	1±1	
4	137.2±1	136.3±1	133.1±2	134.3±3	135 ±2		4.4±1	12 ± 2	13 ±2	11±1	
5	152.8±1	149.0±5	148.5±5		(151)±3	8−, 7	12 ±2	1 ± 0.5	3.5±1		a
		167.6±2						6 ± 2			b
6	180.5±3	180.5±1	180.9±5	281.3±1	181 ±1	4−, 0	5 ±3	47 ± 8	45 ±10	48±10	
7	191.0±1	189.1±1	191.6±2	191.5±1	191 ±1	3+, 3	100 ±4	100 ±10	100 ±15	100±10	
		215.0±2						2.7± 1			c
	230.2±1	251.8±1					0.3±0.1	33 ± 5			d
8	260.4±1	262.8±1		258.0±1	260 ±2	4+, 3	48 ±3	59 ± 6		81± 5	
		285.8±1		275.5±3				40 ± 5		14± 4	e
9	293.6±1	296.4±1		292.3±1	294 ±2	6+, 6	44 ±2	57 ± 6		70± 8	
10	308.2±3	311.5±4		304.3±4	308 ±3	9−, 7	2.7±1	4 ± 2		10± 7	
11	331.7±2	327.3±2		330.0±2	330 ±2	5−, 0	4.1±1	5 ± 2		15± 5	
		341.7±2						13 ± 3			c
12	347.3±1	350.7±2		343.7±3	348 ±2	5+, 3	12 ±2	15 ± 3		16± 4	
		367.1±1		363.8±2				92 ±10		68±20	f
13	370.9±1	376.1±1		373.2±1	373 ±2	4+, 4	169 ±5	187 ±10		173±25	
14	383.3±2	386.3±1			(386)±2		13 ±3	24 ± 6			
15	402.1±2	400.2±1			(401)±2		3.3±1	4 ± 1			
16	422.7±1	418.6±1		421.1±1	421 ±2	7+, 6	48 ±2	23 ± 5		82± 7	
		428.9±1		434.7±3				74 ± 6		13± 5	c
		442.1±2						7 ± 2			g
17	454.5±1	457.6±1		458.7±1	457 ±2	6+, 3	20 ±2	27 ± 6		80±10	
18	468.2±1	467.6±1		470.7±1	469 ±2	5+, 4	52 ±3	55 ±10		63±10	
19	475.5±2	475.7±1			476 ±1		9 ±5	55 ±10			
		489.8±3						3 ± 2			h
20	515.6±1	512.8±2		513.2±1	514 ±1		38 ±6	19 ± 4		78±10	
21	523.8±2	522.6±2		526.0±2	524 ±2		18 ±5	56 ±10		45±10	
		531.2±2						27 ±10			c
22	547.0±1	545.3±1		554.5±1	546 ±2		30 ±4	19 ± 4		80± 7	
23	557.8±1	556.0±1			557 ±2		32 ±3	41 ± 5			
24	571.2±3	565.9±1		573.2±3	(566)±2		7 ±2	42 ± 5		17± 6	
25		578.2±2			(578)±3			9 ± 2			
26	586.3±1	590.9±1		590.8±1	589 ±2		30 ±3	35 ± 6		88±10	
27	596.0±1	601.0±1		603.1±2	(599)±2		42 ±6	70 ± 7		32±10	
28	612.6±4	609.8±1			(610)±2		2.1±1	25 ± 7			

[13] R. A. Kenefick and R. K. Sheline, Phys. Rev. **133**, B25 (1964).

TABLE II. (*continued*)

Level No.	Level energy 45°	Level energy 95°	Level energy (mean)	Intensity 45°	Intensity 95°
29	633.1±1	631.4± 1	632 ±1	16 ±2	26± 3
30	653.8±1	652.6± 2	653 ±1	34 ±3	43±10
31	668.1±1	662.8± 3	668 ±2	8 ±2	18±10
32	690.7±1	691.2± 1	691 ±1	10 ±1	27± 3
33	719.7±1	724.3± 2	721 ±2	10 ±1	21± 4
34	738.0±1	739.4± 1	739 ±1	8 ±1	19± 4
35	767.4±1	767.1± 1	767 ±1	11 ±2	14± 3
	789.1±2			3 ±1	
36	814.2±1	813.7± 1	814 ±1	76 ±4	107± 6
	839.0±1	847.1± 1		82 ±4	15± 2
	862.3±2	874.2± 3		3.4±1	11± 3
37	890.4±1	892.4± 1	891 ±1	60 ±4	92± 7
38	904.8±2	910.5± 3	907 ±3	13 ±2	24± 5
39	923.4±1	925.7± 1	925 ±2	20 ±2	32± 6
40	941.7±3	950.0±11	(942)±3	2.2±1	5± 4
41	960.8±1	960.6± 3	961 ±1	13 ±2	26±10
42	982.2±1	982.4± 1	982 ±1	34 ±2	52± 4
43	1006.6±1	1007.9± 2	1007 ±1	12 ±2	9± 2
44	1035.7±1	1033.3± 1	1035 ±1	10 ±2	21± 2
45	1057.6±1	1055.7± 2	1057 ±1	8 ±1	11± 2
46	1085.1±3	1079.2± 1	1080 ±2	1.7±1	11± 2
47	1103.6±2	1105.1± 1	1105 ±1	4.3±1	18± 3
48	1121.6±1	1123.3± 2	1122 ±2	14 ±2	7± 4
49	1138.6±2	1136.1± 2	1137 ±2	7 ±2	17± 5
50	1153.7±3	1153.8± 4	1154 ±3	3.4±1	18± 5
51	1173.7±1	1171.4± 3	1173 ±1	13 ±2	18± 6
52	1188.1±1	1187.0± 3	1188 ±1	13 ±2	17± 6
53	1205.3±2		(1205)±2	7 ±2	
54	1220.7±2		(1221)±2	5 ±2	
55	1244.7±2		(1245)±2	11 ±2	
56	1268.9±1		(1269)±2	17 ±2	
	1282.8±1	1275.4± 1		15 ±3	39± 6
57	1296.7±1	1295.6± 1	1296 ±1	16 ±3	46± 7
58	1311.8±1	1310.2± 2	1312 ±1	4.7±1	18± 4
59	1335.6±2	1334.2± 3	1335 ±2	12 ±2	17±10
60	1350.6±4	1346.6± 3	1349 ±3	8 ±3	27±10
61	1362.0±3	1360.8± 1	1361 ±1	17 ±3	61± 7
62	1373.1±2	1373.2± 2	1373 ±2	13 ±3	53±10
63	1395.0±1	1399.2± 1	1397 ±2	9 ±2	34± 5
	1412.4±2			8 ±3	
	1427.5±1	1422.2± 2		47 ±5	51±10
64	1440.8±1	1436.5± 1	1439 ±2	31 ±5	100±10
65	1462.7±1	1457.7± 2	1462 ±2	10 ±2	17± 5
66	1486.4±1	1490.0± 3	1487 ±2	8 ±2	22± 7
67	1501.6±2	1504.7± 3	1503 ±2	10 ±2	20± 7
68	1516.9±1	1518.1± 1	1518 ±1	35 ±3	68± 8
69	1536.0±1	1538.4± 1	1537 ±1	31 ±3	67± 9
70	1558.0±1	1559.2± 2	1559 ±1	15 ±2	36± 7
	1573.9±1	1580.4± 1		12 ±2	43± 7
	1589.1±2			9 ±2	
71	1604.5±1	1603.3± 3	1604 ±1	13 ±2	31±10
72	1623.7±1	1619.3± 2	1623 ±2	17 ±2	42±10
73	1641.9±1	1641.1± 1	1642 ±1	21 ±2	55±10
74	1659.4±1	1662.2± 1	1661 ±1	23 ±2	42± 8

[a] A P^{32} impurity peak probably increases the observed intensity at 45°.
[b] This peak may correspond to the (3 −, 0) member of the ground state band.
[c] Unassigned impurity peak.
[d] S^{33} peak at 45°; P^{32} peak at 65°.
[e] Ca^{41} peak at 65°; K^{40} peak at 95°.
[f] Ca^{41} peak at 65°; unassigned impurity at 95°.
[g] P^{32} peak at 65°.
[h] Si^{29} peak at 65°.

equal to the area enclosed by the function outside the data points. The fitting of the first peak as a single level instead of a doublet, although somewhat more difficult, would also be possible. However, previous investigators[4,5] have found an excited state at 191-keV excitation. Taking the peak as a doublet yields a strong

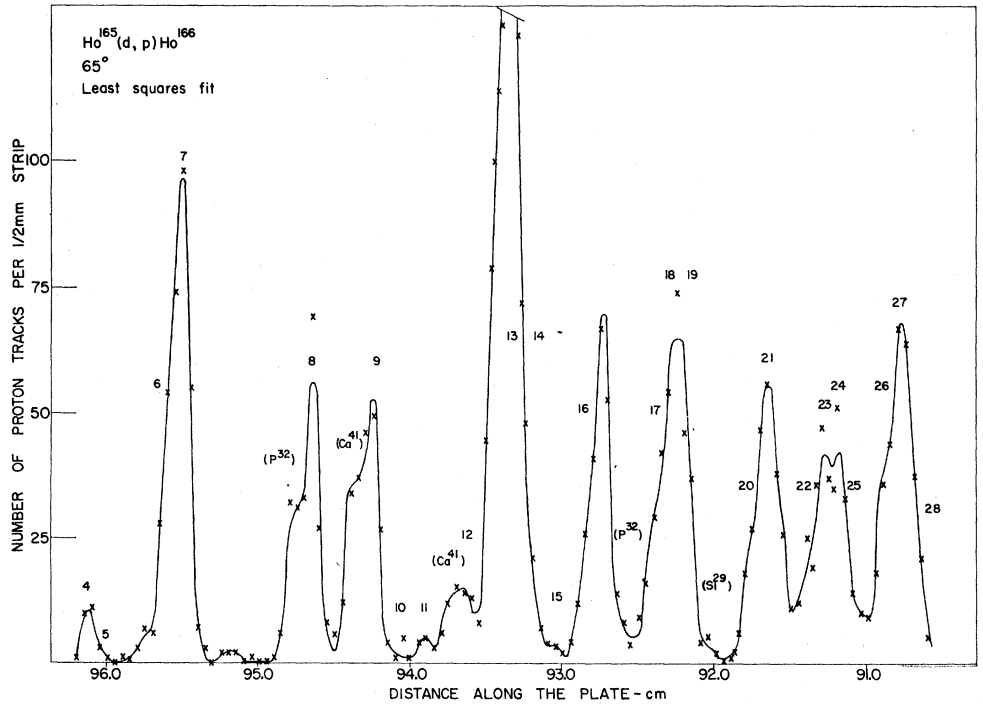

FIG. 2. Least-squares fit of a portion of the 65° spectrum obtained from the reaction Ho^{165}-$(d,p)Ho^{166}$.

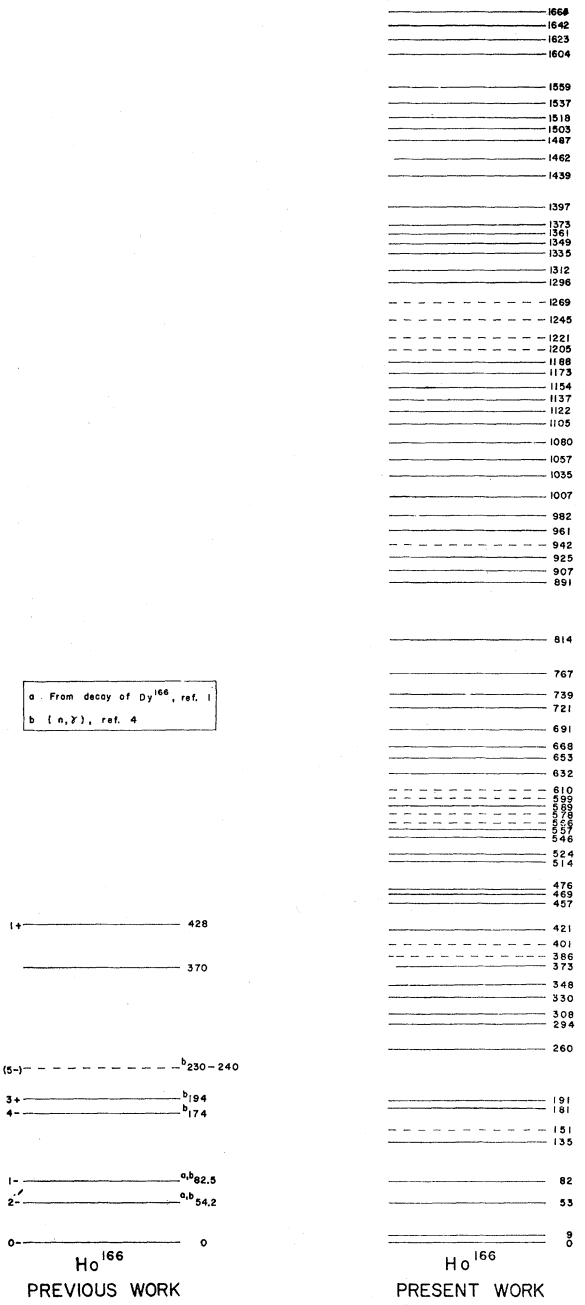

FIG. 3. A comparison of current and previous experimental results for Ho^{166}.

peak at an average excitation energy of 191±3 keV in good agreement with the previous reported data. This is a strong support for the doublet choice.

In Table II information about the levels observed up to 1.661 MeV of excitation is presented. Since the determination of a satisfactory fit is quite subjective, particularly in the graphical analysis, the errors quoted for the peaks under 170-keV excitation are not standard deviations but rather the largest spread in energy compatible with the method used for fitting the peaks. For the other levels, the errors indicated at each angle for energy and intensity correspond to the standard deviation as determined from the least-squares analysis. These errors are too small for two reasons. They do not take into account any error other than those due to ordinary statistics, and in some of the complex structures analyzed, the results depend significantly on the number and width of the fitted peaks. For this reason, the error on the final level sequence is adjusted according to the energy agreement between the different runs. Values between parentheses correspond to doubtful levels. In Fig. 3, a graphical comparison between our results and those of previous investigators[1–5] is given.

IV. COMPARISON OF THEORY AND EXPERIMENT

The theoretical developments necessary to discuss the level structure of odd-odd nuclei has been presented in detail in Sec. II. In order to interpret our spectra using this model, it is necessary to make certain assumptions and approximations beyond those in the model Hamiltonian. First, it is assumed that the effects of H_{INT}, the positions of the single particle states, and inertial parameters cannot be known *a priori* and are therefore taken as free parameters. Second, it is assumed that the most convenient complete orthonormal set of basis vectors that are needed to construct the Hamiltonian matrix is the set (4). Third, it is assumed that only those basis components which appear as states in neighboring isotopes and isotones will make any significant contribution to the state vectors in the low-energy portion of the spectrum. And finally, no attempt is made to take rotation-vibration interaction into account in a quantitative manner.

By choosing Nilsson wave functions[7] to span the Hilbert space of the particles, assumption 3 will presumably be good. Our procedure is first to examine the odd-A isotopes and isotones of the odd-odd nucleus and to construct the Hamiltonian matrix from the basis components observed. Then using the Jacobi iterative method, the matrix is diagonalized and differential cross sections calculated with the state vectors that are obtained. The distorted-wave Born approximation of Bassel, Drisko, and Satchler[8] was used to calculate the differential cross sections. The form for the spectroscopic factor for the rotational model using Nilsson wave functions[7] has been given by Satchler,[14] and MacFarlane and French.[15] However, since a coherent summation must in general be performed when using our model wave functions, care must be exercised to be certain that an acceptable and consistent phasing is adopted both in the diagonalization and in the computation of the spectroscopic factor. In Figs. 4 and 5, the neighboring isotopes and isotones of Ho^{166} are depicted.

[14] G. R. Satchler, Ann. Phys. (N. Y.) **3**, 275 (1958).
[15] M. H. MacFarlane and V. B. French, Rev. Mod. Phys. **32**, 567 (1960).

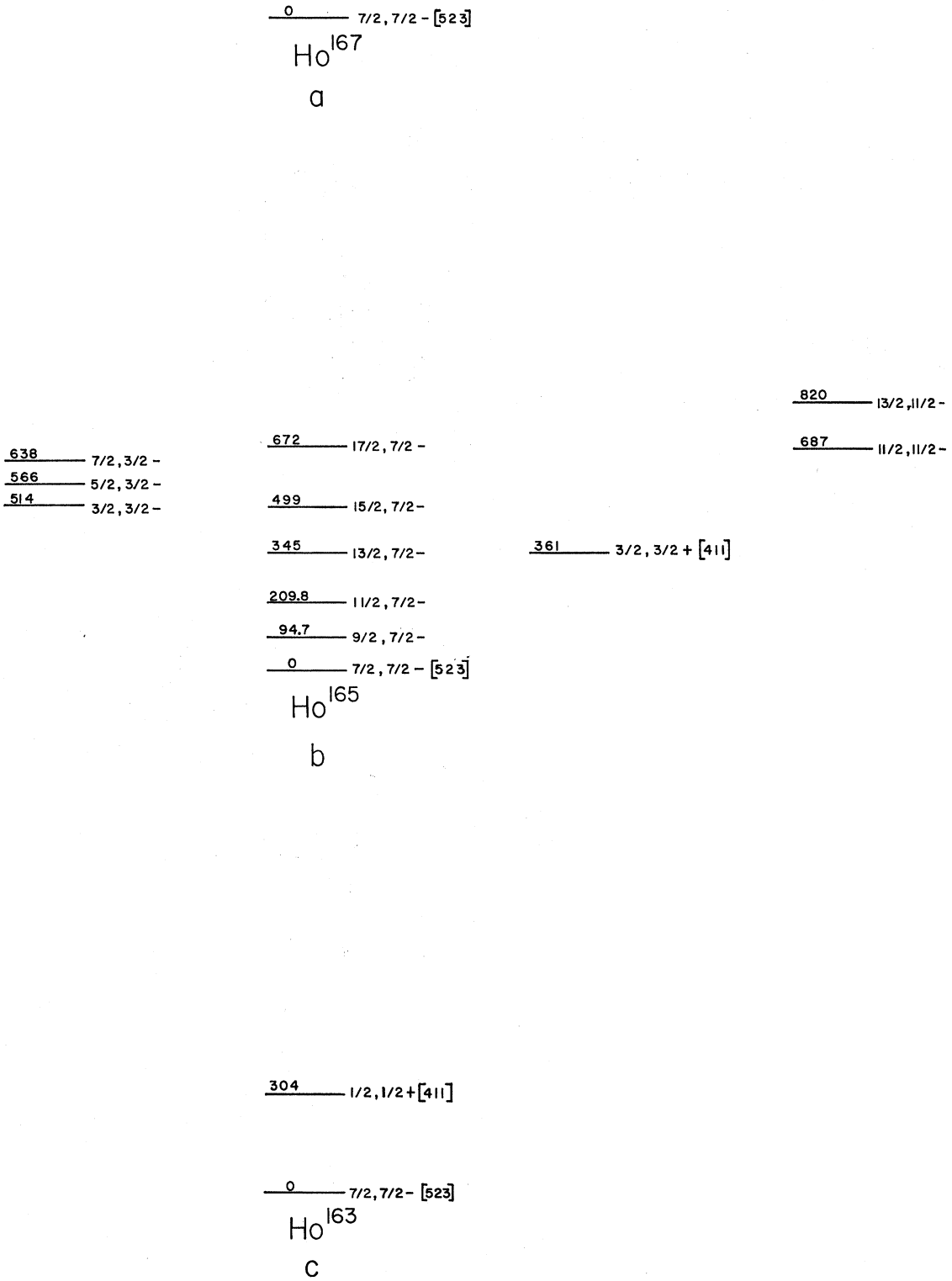

FIG. 4. Levels in odd-A holmium isotopes. The data in parts (a) and (c) are taken from the compilation of B. R. Mottelson and S. G. Nilsson, Kgl. Danske Videnskab. Selskab, Mat.-Fys. Skrifter **1**, No. 8 (1959), while those in part (b) come from the work of R. M. Diamond, B. Elbek, and F. S. Stephens, Nucl. Phys. **43**, 560 (1963).

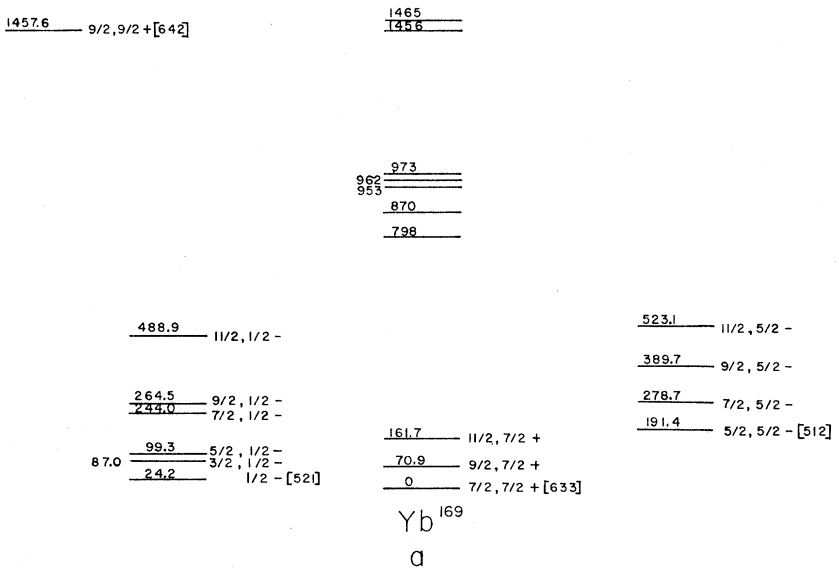

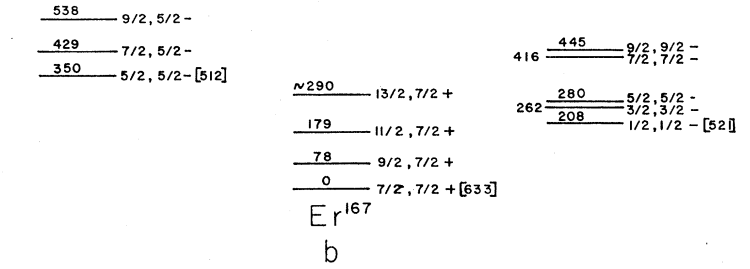

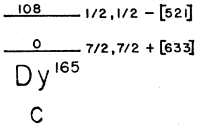

FIG. 5. Levels in odd-A nuclides isotonic with Ho^{166}. The data in part (a) are from the work of R. G. Wilson and M. L. Pool, Phys. Rev. **120**, 1843 (1960); those in part (b) from the work of R. A. Harlan, Dissertation, Florida State University, 1962 (unpublished). Data in part (c) are taken from the compilation of B. R. Mottelson and S. G. Nilsson, Kgl. Danske Videnskab. Selskab. Mat.-Fys. Skrifter **1**, No. 8 (1959).

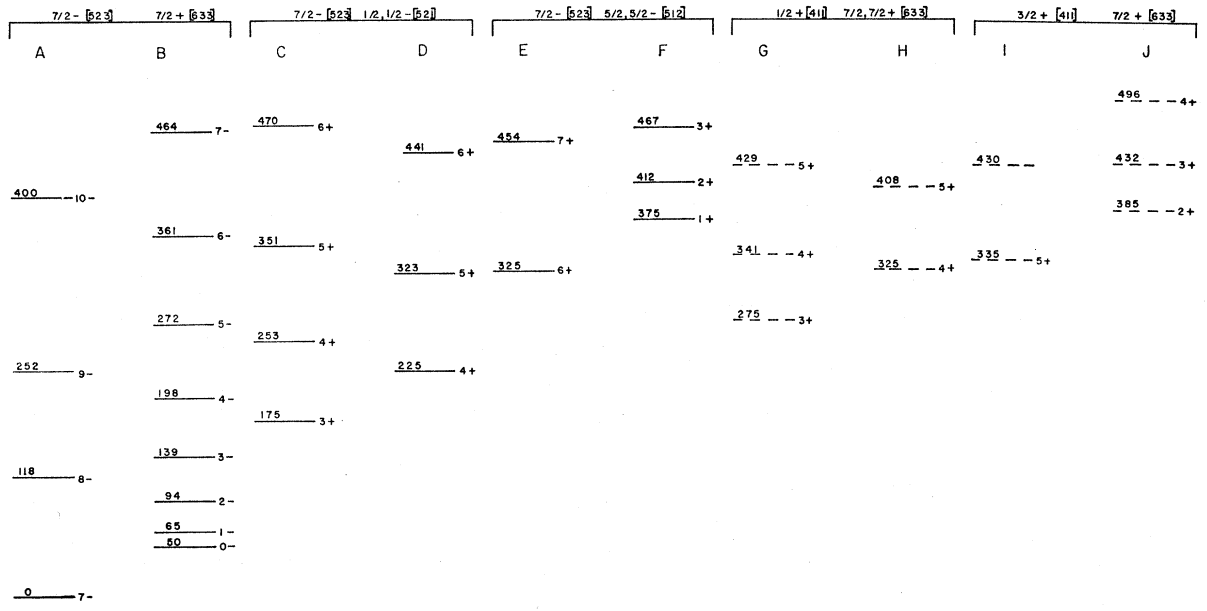

FIG. 6. A predicted level structure for Ho^{166}. Using a simple rotational model the dotted levels are not expected to have any excitation to first order.

With these it is predicted that the complete set of basis components can adequately be approximated by the subset shown in Table III.

TABLE III. Basis vectors for Ho^{166}.

$\phi_1{}^I$	$\psi^-{}_{IM0\ 7/2\ 7/2}$
$\phi_2{}^I$	$\psi^-{}_{IM7\ 7/2\ 7/2}$
$\phi_3{}^I$	$\psi^+{}_{IM3\ 7/2\ 1/2}$
$\phi_4{}^I$	$\psi^+{}_{IM4\ 7/2\ 1/2}$
$\phi_5{}^I$	$\psi^+{}_{IM6\ 7/2\ 5/2}$
$\phi_6{}^I$	$\psi^+{}_{IM1\ 7/2\ 5/2}$
$\phi_7{}^I$	$\psi^+{}_{IM3\ 1/2\ 7/2}$
$\phi_8{}^I$	$\psi^+{}_{IM4\ 1/2\ 7/2}$
$\phi_9{}^I$	$\psi^+{}_{IM5\ 3/2\ 7/2}$
$\phi_{10}{}^I$	$\psi^+{}_{IM2\ 3/2\ 7/2}$

This entire procedure has been programmed for the Florida State University IBM 709 computer. It is not practical to vary the parameters over too wide a range since the computation time is lengthy, approximately one min for a set of parameters. Also a large set of values for the parameters requires a large amount of time to compare experimental data with theoretical results even though the computer is programmed to plot the results for convenient comparison with experimental data. For this reason, we attempted to put rather narrow bounds on the parameter variation. The initial values for the parameters were taken from Fig. 6. This was constructed by choosing excitation energy estimates for the band heads from data on neighboring odd-A nuclei. Further we assumed that the splitting between the band heads of a given configuration is 50 keV and that their relative orientation obeys the coupling rules of Gallagher and Moszkowski.[16] We assumed that the moment of inertia for the two unperturbed bands that arise from the same configuration is the same, and we obtained an estimate for that moment of inertia as follows.

The values of $\hbar^2/2\mathfrak{F}$ are averaged for the ground-state rotational bands for all even-even nuclei with mass 166. Then the moments of inertia for rotational bands built on the Nilsson proton orbital in question are examined. It is convenient to define a quantity

$$\delta_p=\mathfrak{F}_{o-e}-\mathfrak{F}_{e-e}, \tag{21}$$

where $\mathfrak{F}_{e-e}$ is the average value of $\mathfrak{F}$ for all even-even nuclei with mass 166, and $\mathfrak{F}_{o-e}$ is the value of $\mathfrak{F}$ for an odd-A isotope of holmium. Similar considerations for the odd neutron lead to the definition

$$\delta_n=\mathfrak{F}_{e-o}-\mathfrak{F}_{e-e}. \tag{22}$$

The values of $\mathfrak{F}_{e-e}$ and $\mathfrak{F}_{o-e}$ are, of course, based on experimental data from odd-A nuclei. Preferably they are taken from the isotopic and isotonic nucleus that is nearest in mass to $A=166$ and has a band head with excitation energy approximately the same as the band head in Ho^{166}. Then

$$\mathfrak{F}_{o-o}=\mathfrak{F}_{e-e}+\delta_p+\delta_n. \tag{23}$$

The inertial parameter which we shall call a_{o-o} ($a_{o-o}=\hbar^2/2\mathfrak{F}_{o-o}$) for the two rotational bands constructed with the two Nilsson orbitals in question can then be

[16] C. J. Gallagher and S. A. Moszkowski, Phys. Rev. 111, 1282 (1958).

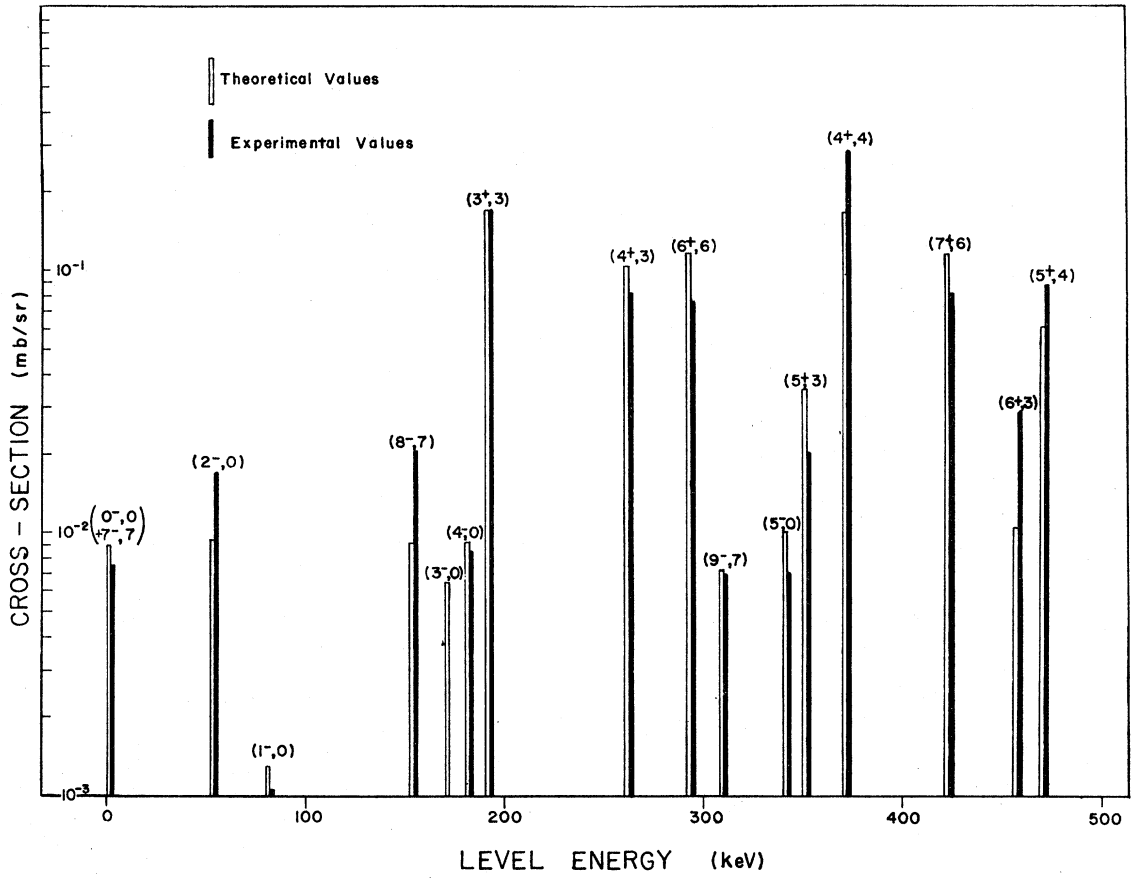

FIG. 7. A comparison of experimental and theoretical cross sections for Ho^{166} at 45°. Because the ground-state doublet is so weakly excited at this angle, a meaningful analysis of this structure is impossible. Thus we have added both the experimental and theoretical intensities and represent the sum as the ground state. The experimental cross sections have been obtained by normalizing the relative intensities so that the 191-keV level has the theoretical cross section for the $I\pi K=3+3$ state.

TABLE IV. Properties of theoretically predicted states in Ho^{166}. (Energies in keV.)

Level No.	Spin	Parity	E_{ex} Exp.	E_{ex} Theory	First-order energy[a]	a_{0-0} for band[a]	B[a]	Cross section (mb/sr)	$\phi_1{}^I$	$\phi_2{}^I$	Wave function $\phi_3{}^I$	$\phi_4{}^I$	$\phi_5{}^I$
0	0	−	0	0	0[b]	9.0[b]	−32	3.39×10^{-5}	1.0				
1	7	−	9	9	9[b]			4.82×10^{-3}		1.0			
2	2	−	53	54				3.95×10^{-3}	1.0				
3	1	−	82	82				1.29×10^{-3}	1.0				
5	8	−	151	153				9.18×10^{-3}		1.0			
5a	3	−		172				6.61×10^{-3}	1.0				
6	4	−	181	180				9.20×10^{-3}	1.0				
7	3	+	191	191	191[b]	9.5[b]		1.69×10^{-1}			1.0		
8	4	+	260	261				1.02×10^{-1}			0.972	−0.234	
9	6	+	294	294	294[b]	9.1[b]		1.17×10^{-1}					1.0
10	9	−	308	315				7.28×10^{-3}		1.0			
11	5	−	330	334				1.08×10^{-2}	1.0				
12	5	+	348	350				3.51×10^{-2}			0.947	−0.322	
13	4	+	373	373	367[b]			1.66×10^{-1}			0.234	0.972	
16	7	+	421	421				1.15×10^{-1}					1.0
17	6	+	457	458				1.06×10^{-2}			0.925	−0.381	
18	5	+	469	474				6.11×10^{-2}			0.322	0.947	

[a] Given only for the band head.
[b] This number was used as a free parameter.

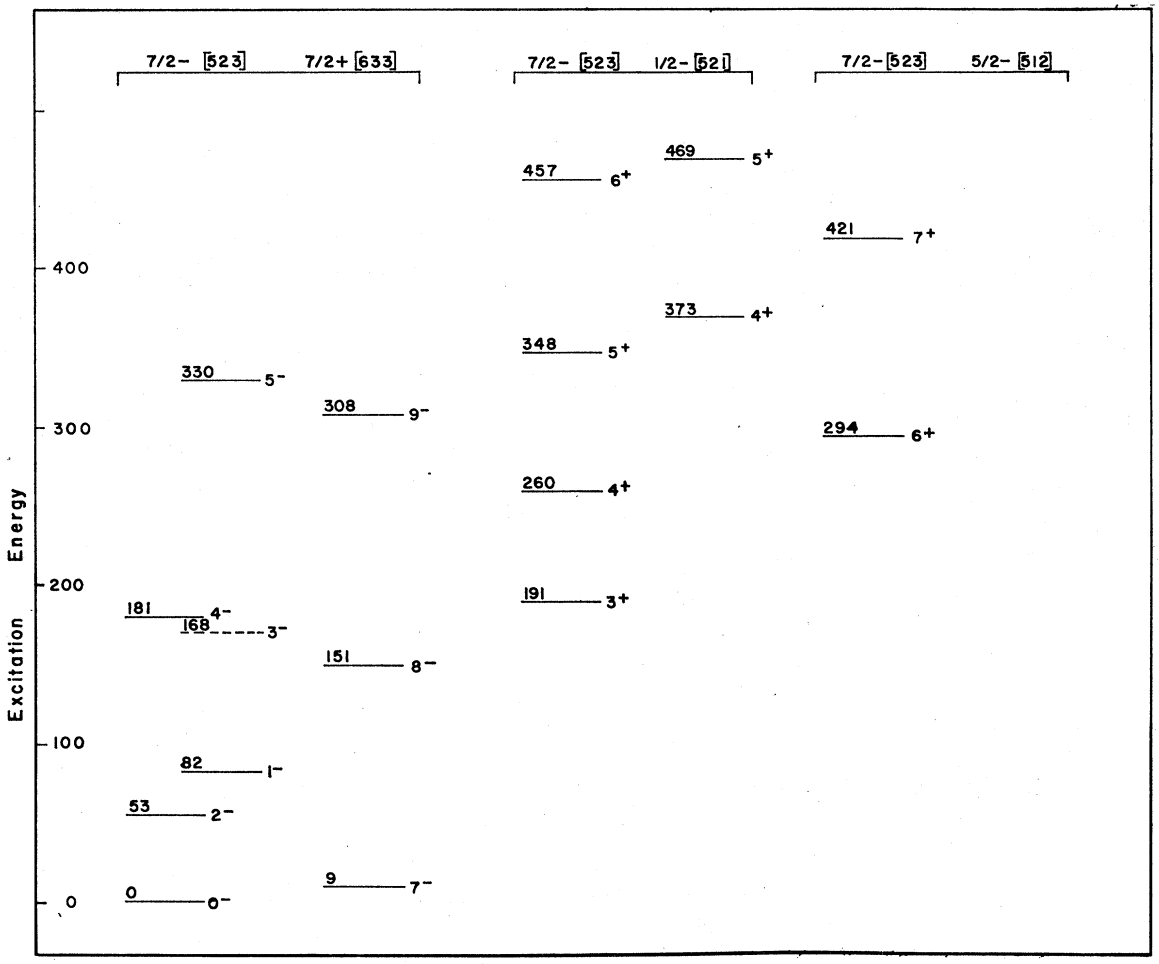

FIG. 8. The schematic presentation of our interpretation of the experimental levels.

written

$$a_{o-o}=\frac{a_{e-e}a_{e-o}a_{o-e}}{a_{e-e}a_{e-o}+a_{e-e}a_{o-e}-a_{e-o}a_{o-e}}. \quad (24)$$

In Fig. 7 and Table IV, the "best" results that can be obtained with the theory are presented. The states in the figure are numbered to correspond to the levels of the spectrum in Sec. III and the information given in Table IV.

Although there is weak experimental evidence for the existence of $I\pi K=3-0$ state, its cross section is much less than that predicted theoretically, and so the experimental state is not shown in Fig. 7. Because the energy agreement is so good, the experimental cross sections have been systematically placed to the right of the theoretical quantity. In Fig. 8, an analysis of the experimental data is presented where it is broken into bands.

A comparison of Fig. 6 and Fig. 8 shows that all the neutron excited levels expected to be observed at the bottom of the scheme have been disclosed. The main differences are that the 0− state is lower than the 7− state and forms the ground state. Further, the splitting of the 3+ and 4+ band heads formed on the $\frac{7}{2}-[523]$, $\frac{1}{2}-[521]$ configuration is about 180 keV. Finally, in the $\frac{7}{2}-[523]$, $\frac{5}{2}-[512]$ configuration, the $K=6$ band has been excited, but the $K=1$ band has not yet been observed. The 435-keV 1+ level found in the decay of[3] Dy^{166} cannot be identified with this missing level. The log ft of the β branch feeding it has been measured to be 4.9. This small value indicates that there is no change in the asymptotic quantum numbers [523] of the decaying state. The 435-keV level corresponds then to the $\frac{7}{2}-[523]$, $\frac{5}{2}-[523]$ hole neutron excited state, a state which is not expected to be excited in a (d,p) reaction.

All the certain levels which we have observed up to 470 keV have been given a reasonable assignment, with the sole exception of the weak 135-keV peak.

V. CONCLUSION

This work has been primarily concerned with the determination of energy levels in the odd-odd nucleus

Ho^{166}. In order to give possible interpretations of these data it was necessary to develop a mathematical model. For this purpose the model of Bohr, Mottelson,[9] Nilsson,[7] and Kerman[10] has been extended to describe explicitly two nucleons outside a spheroidal core. By neglecting certain terms in the Hamiltonian, it was possible to separate the problem and obtain a direct product basis with which to construct the Hamiltonian matrix. For purposes of comparing our data with theory, moments of inertia and those parts of the matrix elements which depend on the proton-neutron interaction are taken as free parameters. These parameters were allowed to vary over reasonable ranges, and for each parameter set the Hamiltonian matrix was diagonalized. With the resulting energies and wave functions, a level diagram was constructed and using a distorted-wave Born approximation,[8] a theoretical (d,p) spectrum predicted. From the parameterized wave functions which gave the best fit, it has been possible to draw some conclusions about the nuclear structure. The validity of these conclusions is somewhat hard to assess because of the many physical approximations incorporated in the mathematical model. Nevertheless, the agreement between theory and experiment has been encouraging.

The most obvious theoretical extension of this work is to study the effects of H_{INT} using both central and tensor components for the residual interaction. This is currently being done. Then the most important step to be taken is to correlate our data with the results of precision (n,γ) experiments. When complete and unambiguous agreement is found between the two experiments, it should be possible to have a great deal of confidence about the exact nature of the levels and to put various structure models to some severe tests.

ACKNOWLEDGMENTS

The authors wish to express their indebtedness to Dr. Henry Motz who spent a great deal of time helping develop the least-squares analysis technique and to Dr. Merle Bunker who pointed out the argument against the 435-keV level coming from the $\frac{7}{2}-[523]$, $\frac{5}{2}-[512]$ configuration.

PHYSICAL REVIEW VOLUME 137, NUMBER 4B 22 FEBRUARY 1965

Nuclear Magnetic Moment of Pr^{141} from the Hyperfine Structure of Doubly Ionized Praseodymium

JOSEPH READER AND JACK SUGAR
National Bureau of Standards, Washington, D. C.
(Received 21 September 1964)

The hyperfine structure in the spectrum of doubly ionized Pr^{141} was observed by means of a sliding spark discharge and a concave-grating spectrograph. Measurements of the hyperfine patterns resulted in a value for the splitting factor of the $6s$ electron of $a_{6s}=+0.639\pm0.007$ cm^{-1}. The probability density of the $6s$ electron at the nucleus was calculated by using interpolated values of the energy difference and quantum defect difference for the $4f^26s$ and $4f^27s$ configurations. Application of the Goudsmit-Fermi-Segrè formula yields a value for the nuclear magnetic moment $\mu_I=+4.09\pm0.06$ nm. The various contributions to the stated uncertainties are discussed in detail.

I. INTRODUCTION

THERE has been considerable uncertainty regarding the nuclear moment of Pr^{141}. Measurements made by various workers on the hyperfine structure of *neutral*, *singly ionized*, and *triply ionized* Pr have yielded values of μ_I ranging from 3.8 to 5.1 nm. No direct measurement of the Pr^{141} nuclear moment has yet been made.

The uncertainties and discrepancies in the results arise mainly from an inability to calculate reliably the strength of the magnetic field at the nucleus produced by orbital electrons in unfilled shells. In the case of an s electron, this field is proportional to $\psi^2(0)$; for an electron with $l>0$, the field is proportional to the average value of $1/r^3$. Because of the lack of complete analyses of the spectra of neutral Pr and its ionic species, these electronic quantities cannot be determined from the known Pr energy levels. This situation is common to many of the rare earths.

Recently an extensive analysis of the spectrum of *doubly ionized* Pr was reported.[1] As a result of this analysis and subsequent work, 22 of the 24 theoretically possible levels of the $4f^26s$ configuration are known. Also, 81 higher levels belonging to $4f^26p$ and $4f5d^2$ are known. These levels combine strongly with the $4f^26s$ levels to give a large number of lines showing wide hyperfine splittings. We have measured the hyperfine structure (hfs) of these lines and have obtained a value for the splitting factor a_{6s}. We have also derived an accurate value for $\psi^2(0)$ based on the behavior of the $4f^Nns$ series $(n=6,7,8)$ of several rare-earth ions. With these results a new experimental value for $\mu_I(Pr^{141})$ could be obtained.

[1] J. Sugar, J. Opt. Soc. Am. **53**, 831 (1963).